

Regular and quasi black hole solutions for spherically symmetric charged dust distributions in the Einstein–Maxwell theory

Dubravko Horvat, Saša Ilić and Zoran Narančić

Department of Physics, Faculty of Electrical Engineering and Computing, University of Zagreb, Unska 3, HR-10 000 Zagreb, Croatia

E-mail: dubravko.horvat@fer.hr, sasa.ilijic@fer.hr

Abstract. Static spherically symmetric distributions of electrically counterpoised dust (ECD) are used to construct solutions to Einstein-Maxwell equations in Majumdar–Papapetrou formalism. Unexpected bifurcating behaviour of solutions with regard to source strength is found for localized, as well as for the delta-function ECD distributions. Unified treatment of general ECD distributions is accomplished and it is shown that for certain source strengths one class of regular solutions approaches Minkowski spacetime, while the other comes arbitrarily close to black hole solutions.

PACS numbers: 04.40.Nr

1. Introduction

Static bodies resulting from combined gravitational attraction and electrical (electrostatic) repulsion have been playing a central role in many investigations, eg. [1, 2, 3] and references therein, connected with general relativistic treatment of gravitational contraction. As a part of Einstein equation, one has to specify energy-momentum tensor which, for a perfect fluid, has the form

$$T_{\mu\nu} = (\rho + p) u_\mu u_\nu + p g_{\mu\nu}, \quad (1)$$

where ρ , p , u^μ and $g_{\mu\nu}$ are mass density, pressure, four-velocity and metric (in geometrized units: $G = 1 = c$). In addition, one has to specify the equation of state relating the pressure to the density $p = p(\rho)$. According to the Oppenheimer-Snyder scenario [4], in a static spherically symmetric perfect fluid ball with the above energy momentum tensor, after stationary phase and at the end of nuclear burning, the central pressure is no longer able to counterbalance the gravitational attraction and the ball starts to collapse. By setting $p = 0$ the energy momentum tensor assumes the form characteristic for dust ball $T_{\mu\nu} = \rho u_\mu u_\nu$. Eventually, as the ball shrinks one can expect formation of a black hole.

The Majumdar–Papapetrou formalism [5, 6, 7, 8] can be applied to study properties of spacetimes generated by $T_{\mu\nu} = \rho u_\mu u_\nu$ where ρ represents static electrically counterpoised dust (or extremal charged dust, ECD), i.e. pressureless matter in equilibrium under its own gravitational attraction and electrical repulsion [1, 2, 3]. Special attention has been paid to ECD distributions leading to spacetimes that are regular everywhere, but with exterior arbitrarily close to that of an extremal Reissner–Nordström (ERN) black hole [9, 10, 11].

This paper considers the coupled Einstein-Maxwell field equations in the Majumdar–Papapetrou approach. With the energy-momentum tensor given by (1) with $p = 0$, our study will concentrate on diverse (analytic) spherically symmetric forms of ECD distributions and corresponding solutions will be found. The theoretical framework is presented in section 2. In section 3, we present the static solutions to Einstein-Maxwell equations for diverse ECD distributions obtained numerically, and in section 4 for the δ -shell distribution, all of which show interesting bifurcating properties. In section 5, we discuss the bifurcating behaviour and show that diverse distributions can be treated on equal footing. Similar behaviour found in gauge theories and Einstein–Yang–Mills systems is discussed, and we give some details on numerical methods for finding bifurcating solutions. In section 6, we show that with adjusting of the source strength and appropriate rescaling of the solutions, the spacetimes with exteriors arbitrarily close to the ERN case can be obtained. Conclusions are given in section 7, and extension of the present work is proposed.

2. Theoretical framework

One usually starts by defining a static spherically symmetric line element of the form

$$ds^2 = -B(r) dt^2 + A(r) dr^2 + r^2 d\omega^2, \quad (2)$$

where $d\omega^2 = d\vartheta^2 + \sin^2 \vartheta d\varphi^2$. For an asymptotically flat spacetime, one requires

$$A(r)|_{r \rightarrow \infty} = B(r)|_{r \rightarrow \infty} = 1, \quad (3)$$

and for a nonsingular spacetime $A(r=0) = 1$. Papapetrou has shown [6, 7] that the line element can be written as

$$ds^2 = -e^\chi dt^2 + e^\varphi (dX^2 + dY^2 + dZ^2) \quad (4)$$

and that it is possible to connect functions χ and φ in such a way as to satisfy (as one possibility) $d\chi/d\varphi = -1$ or $\chi(\varphi) = -\varphi$. Together with Majumdar's assumption [5] about connection between g_{tt} (or g_{00}) metric component and a scalar component of the electromagnetic potential A^μ comprising the electromagnetic energy-momentum tensor $T_{\mu\nu}^{(\text{em})}$, the line element ds^2 in the Majumdar–Papapetrou form can be written in the harmonic coordinates (t, \mathbf{X}) as

$$ds^2 = -e^{-\varphi} dt^2 + e^\varphi (dX^2 + dY^2 + dZ^2) \quad (5)$$

(in the original notation of [7]). We will assume the spherical symmetry as a general symmetry requirement for our problem. The essential ingredient to the line element (5), as shown by Majumdar, are additional assumptions which should be made about a specific form for the energy-momentum tensor $T_{\mu\nu}$ that enters the Einstein equations

$$R_{\mu\nu} - \frac{1}{2} g_{\mu\nu} R = 8\pi T_{\mu\nu} \quad (6)$$

(in geometrized units). The component of $T^{\mu\nu}$ due to electromagnetic fields is given by

$$T_{\mu\nu}^{(\text{em})} = F_\mu{}^\sigma F_{\nu\sigma} - \frac{1}{4} g_{\mu\nu} F^{\rho\sigma} F_{\rho\sigma}, \quad (7)$$

where $F_{\mu\nu} = A_{\nu,\mu} - A_{\mu,\nu}$ is the antisymmetric electromagnetic field tensor, comma denoting the ordinary derivative to differ from semicolon denoting the covariant derivative. It satisfies the empty space equation $F^{\mu\nu}{}_{;\nu} = 0$.

A more general situation differing from the one described above corresponds to

$$T_{\mu\nu} = T_{\mu\nu}^{(\text{em})} + T_{\mu\nu}^{(\text{m})}, \quad (8)$$

where the superscript (m) denotes matter. The absence of $T_{\mu\nu}^{(\text{m})}$ leads to Reissner–Nordström solutions with $B(r) = A(r)^{-1} = (1 - 2m/r + q^2/r^2)$ for $A^0 = e/r$. It is shown in Ref. [12] that for charged sphere of radius a , for r large enough, m could be set equal to zero, whereas for the interior solution, i.e. $r < a$, one is not permitted to put $m = 0$. It follows that electric charge contributes to the gravitational mass of the system. In addition, mass as given in $B(r) = A(r)^{-1}$ above satisfies a positivity condition $m > 0$. Citing Ref. [12] ‘a charged sphere must have a positive mass’.

In the case of the complete $T^{\mu\nu}$ given in (8) one assumes also a perfect fluid of classical hydrodynamics for which, in general, energy-momentum tensor is given by (1).

With $p = 0$, the energy momentum tensor (1) reduces to $T_{\mu\nu}^{(m)} = \rho u_\mu u_\nu$, where ρ is now an invariant dust density and u_μ is the four-velocity which will be assumed to be in non-moving (co-moving) coordinate system so that

$$u^\mu = \frac{dX^\mu}{ds} \longrightarrow u^\mu = \delta_0^\mu (-g_{00})^{-1/2}. \quad (9)$$

The electromagnetic part of $T_{\mu\nu}$ is given, as before, with (7). The four-current density of the the charge/matter/dust distribution is given by

$$J^\mu = \rho_e u^\mu. \quad (10)$$

At this point, the crucial assumption is made by setting the electric charge density ρ_e equal to the matter density ρ , or somewhat more general $\rho_e = \pm\rho$. Now the metric (5) can be written in the form

$$ds^2 = -U^{-2} dt^2 + U^2 (dX^2 + dY^2 + dZ^2). \quad (11)$$

The Einstein field equations incorporating the above introduced ingredients are given by

$$\begin{aligned} G_{\mu\nu} &= 8\pi (T_{\mu\nu}^{(em)} + T_{\mu\nu}^{(m)}) \\ &= 8\pi \left[\frac{1}{4\pi} \left(F_\mu{}^\sigma F_{\nu\sigma} - \frac{1}{4} g_{\mu\nu} F^{\rho\sigma} F_{\rho\sigma} \right) + \rho_e u_\mu u_\nu \right], \end{aligned} \quad (12)$$

and by using the Majumdar (or Majumdar–Papapetrou) assertion, the generalized (nonlinear) Poisson equation (with $\rho = \rho_e$)

$$F^{\mu\nu}{}_{;\nu} = 4\pi J^\mu = 4\pi \rho u^\mu \quad (13)$$

assumes a simple form

$$\nabla^2 U = -4\pi \rho U^3. \quad (14)$$

Here U and ρ are functions of the co-moving coordinates (X, Y, Z) determined from the zeroth component of the electromagnetic potential A^μ , i.e.

$$A^\mu = \delta_0^\mu \phi \quad \text{and} \quad U = \frac{1}{1 - \phi}. \quad (15)$$

Confining our attention to the spherically symmetric case, the Majumdar–Papapetrou metric can be written as

$$ds^2 = -U^{-2}(R) dt^2 + U^2(R) (dR^2 + R^2 d\Omega^2). \quad (16)$$

The metric function U is a function of R only, so (14) reduces to

$$\nabla^2 U(R) = R^{-2} (R^2 U'(R))' = -4\pi \rho(R) U^3(R), \quad (17)$$

where the prime denotes the differentiation with respect to R . The line element (16) can be expressed in the standard form (2) through the coordinate transformation

$$r = RU(R), \quad (18)$$

with the following relations among the profile functions:

$$B(r) = U^{-2}(R) \quad (19)$$

and

$$\frac{1}{\sqrt{A(r)}} = 1 + \frac{R}{U(R)} \frac{dU(R)}{dR}. \quad (20)$$

In regions of space where $\rho(R) = 0$, the nonlinear equation (17) reduces to a homogeneous equation with the general solution

$$U(R) = k + \frac{m}{R}, \quad (21)$$

where k and m are integration constants. Using (18)–(20), to express the line element in the standard form (2), one obtains $B(r) = A(r)^{-1} = k^{-2} (1 - m/r)^2$. If the region of space we are considering extends to $r \rightarrow \infty$, according to the requirements (3), we set $k = 1$, and only m remains as a free parameter. The line element is then

$$ds^2 = - \left(1 - \frac{m}{r}\right)^2 dt^2 + \left(1 - \frac{m}{r}\right)^{-2} dr^2 + r^2 d\omega^2, \quad (22)$$

which we recognize as the extremal Reissner–Nordström (ERN) spacetime. The general Reissner–Nordström (RN) solution specifies the asymptotically flat spacetime metric around an electrically charged source. Expressing the RN line element in the standard form (2), one has $B(r) = A(r)^{-1} = (1 - 2m/r + q^2/r^2)$, where m and q are the ADM mass and charge of the source. For $m < q$, the RN spacetime is regular everywhere except at $r = 0$, while for $m > q > 0$, in addition to the singularity at $r = 0$, it exhibits two horizons located at $r = m \pm (m^2 - q^2)^{1/2}$. In the ERN case, i.e. $m = q$ (gravitational attraction balances electrical repulsion), only one horizon at $r = m$ is present. It is important to note that the solution (21) is valid in the range $0 \leq R < \infty$ which is according to eq. (18) mapped to $m \leq r < \infty$. That is to say that the solution (21) specifies only the external part of the ERN spacetime (see [10]).

We shall proceed to solve the field equation (17) for several distributions of electrically counterpoised dust (or extremal charged dust, ECD) $\rho(R)$. The ECD distributions that will be considered effectively vanish at large R , so we expect our spacetimes to behave like (22) for $R \rightarrow \infty$. The parameter $m_\infty = R(U - 1)|_{R \rightarrow \infty}$, characterizing the asymptotic behaviour of $U(R)$ at large R , is the ADM mass seen by the distant observer. The behaviour of $U(R)$ as $R \rightarrow 0$ can be characterized by the parameter $m_0 = RU|_{R \rightarrow 0}$. The metric (16) is regular at $R = 0$ only if $m_0 = 0$ and, according to (18), the range $0 \leq R < \infty$ is mapped to $0 \leq r < \infty$. On the other hand, if $m_0 > 0$ the function $U(R)$ is infinite at $R = 0$ which indicates the singularity. As the range $0 \leq R < \infty$ is now mapped to $m_0 \leq r < \infty$, this singularity is, in the r -coordinate, located at $r = m_0$. Therefore, we may understand the parameter m_0 as the ‘mass below horizon’. If $\rho = 0$ we have $m_0 = m_\infty$, while in case of non-vanishing ECD density ρ we have

$$m_\infty = m_0 + m_\rho, \quad (23)$$

where m_ρ can be understood as the contribution of ECD to the ADM mass of the configuration. The ‘ECD mass’ m_ρ is the space integral of the ECD density ρ :

$$m_\rho = 4\pi \int_0^\infty \rho U^3 R^2 dR = 4\pi \int_{m_0}^\infty \rho A^{1/2} r^2 dr. \quad (24)$$

We conclude this Section by pointing out, for later convenience, that if certain $U(R)$ and $\rho(R)$ solve the equation (17), one is allowed to rescale the functions

$$\begin{aligned} U(R) &\longrightarrow U^*(R) = U(\alpha R), \\ \rho(R) &\longrightarrow \rho^*(R) = \alpha^2 \rho(\alpha R), \end{aligned} \quad (25)$$

which, as a consequence, rescale the mass parameters according to

$$m \longrightarrow m^* = m/\alpha. \quad (26)$$

These relations will help us compare field configurations corresponding to different mass parameters.

3. General ECD distributions and bifurcating solutions

Our approach in constructing solutions to the Majumdar–Papapetrou systems is to assume certain ECD distribution $\rho(R)$ and then integrate the differential equation (17) numerically to obtain the metric function $U(R)$, and is therefore different from the approach used in [1, 10] where $\rho(R)$ is analytically reconstructed from the assumed metric and the requirement that $\rho(R)$ may not be negative. At the expense of requiring numerical procedures our approach allows complete freedom in choosing the shape of $\rho(R)$, which we found more natural. However, in accord with the requirement that our solutions be asymptotically flat, we choose ECD distributions $\rho(R)$ that are well localized in the R -coordinate. More specifically, we require that the total mass/charge in a linear theory $4\pi \int_0^\infty \rho R^2 dR$ is finite, i.e. that $\rho(R)$ falls off more rapidly than $1/R^3$. As our first example we take $\rho(R)$ of the form

$$\rho(R) = \frac{\eta}{24\pi} (R/\tilde{R}) e^{-R/\tilde{R}}, \quad (27)$$

where \tilde{R} is the length scale that in further text we set equal to 1, η has the role of an adjustable source strength factor (in appropriate units) and 24π is a normalization constant that renders $4\pi \int_0^\infty \rho R^2 dR = 1$ for $\eta = 1$ and $\tilde{R} = 1$.

As (17) is a second order differential equation we have to impose two boundary conditions onto a solution. As the first boundary condition, we use the requirement that the spacetime is asymptotically flat, i.e. $U|_{R \rightarrow \infty} = 1$, and as the second we chose to fix the parameter $m_0 = R U|_{R \rightarrow 0}$. We obtain the solutions by numerical integration [13] of the differential equation. Starting with the solution of (17) for source strength $\eta = 0$, i.e. $m_\infty = m_0$, we slowly increase the value of η . Increasing of η evolves the solution toward $m_\infty > m_0$, but one may only increase the value of η up to a critical value η_c . The dependence of m_∞ on η in solutions obtained in this way is shown as the lower part of the solution tracks in figure 1. The critical points are labeled (a), (d), (g), and (h), and the corresponding values of η_c and m_∞ are given in table 1.

In addition to these solutions there exists another class of solutions: starting from a critical solution, i.e. one obtained with η_c , in our numerical procedure, we could require a slight increase in m_∞ and allow the source strength η to adjust itself freely. The solutions to the differential equation can be found and it turns out that, for this

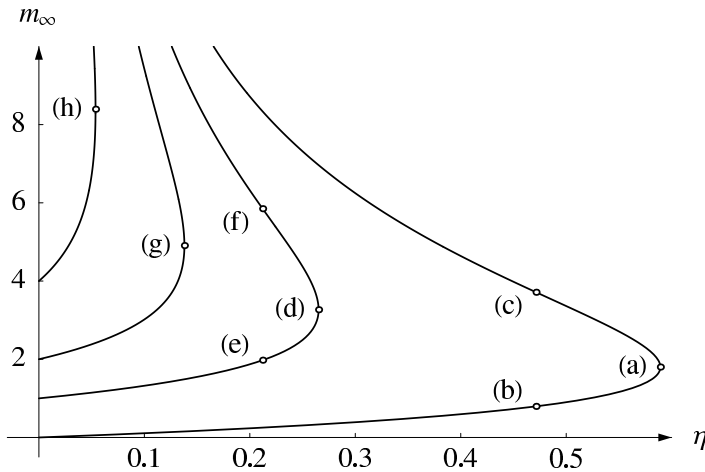


Figure 1. The dependence of m_∞ (ADM mass) on source strength η in solutions to (17) with ECD distribution given by (27) and boundary conditions $m_0 = 0$ (leading to regular spacetimes) and $m_0 = 1, 2, 4$ (leading to singular spacetimes). The numerical values of η and m_∞ for the solutions labeled by letters (a)–(h) are given in table 1.

Table 1. Numerical values of η and m_∞ for the solutions labeled by letters in figure 1.

m_0	η_c	$m_\infty(\eta_c)$	$m_\infty^-(\frac{4}{5}\eta_c)$	$m_\infty^+(\frac{4}{5}\eta_c)$
0	0.589 272	1.801 05 (a)	0.795 196 (b)	3.713 25 (c)
1	0.265 212	3.266 61 (d)	1.976 69 (e)	5.849 51 (f)
2	0.137 966	4.906 04 (g)		
4	0.053 701	8.394 04 (h)		

class of solutions, as we increase m_∞ , the source strength η decreases! These solutions are indicated as the upper part of the tracks in the m_∞ versus η diagram (figure 1). Therefore, for source strength $\eta > \eta_c$ there appears to be no solution to (17) that is asymptotically flat, while if starting from η_c (i.e., from the critical solution such as (a) or (d) in figure 1), the solutions bifurcate by following either lower (through points (b) or (e)) or upper m_∞ -branch (through points (c) or (f)). This kind of bifurcation is of the ‘turning point type’ as explained in [14] (see also [15]).

In figure 1, the critical point on the curve corresponding to the boundary condition $m_0 = 0$ is obtained with $\eta_c = 0.589 27$ and is labeled (a). The points (b) on the lower and (c) on the upper m_∞ -branch indicate the two independent solutions obtained with $\eta = \frac{4}{5}\eta_c = 0.471 41$. The corresponding masses are given in table 1. The components of the metric in the r -coordinate $A(r) = g_{rr}$ and $B(r) = g_{tt}$ for the solutions labeled (a)–(c), are shown in figure 2. At large r , the metric components $A(r)$ and $B(r)$ coalesce into the ERN metric (22). But in contrast to the ERN metric, $A(r)$ and $B(r)$ of our solutions are finite at all r so the spacetime does not involve an event horizon. This is true for all solutions obtained with the boundary condition $m_0 = 0$. We call them the regular solutions, although in section 6 we show that these solutions may come arbitrarily close to having an extremal horizon.

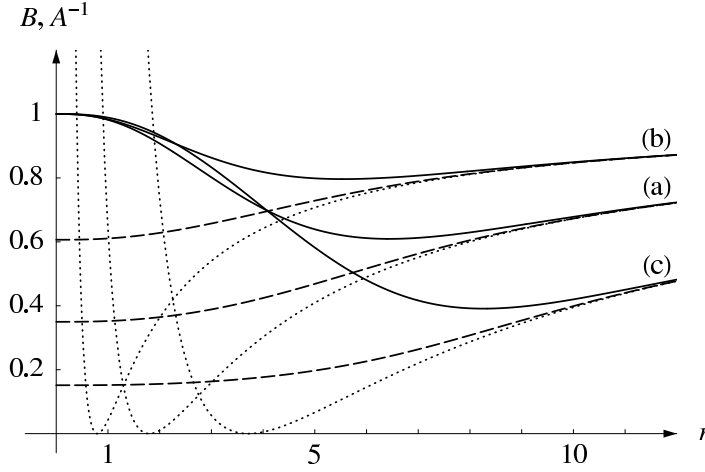


Figure 2. Regular spacetime metric components $g_{rr}^{-1} = A^{-1}(r)$ (thick lines) and $g_{tt} = B(r)$ (dashed lines) obtained by solving the field equation (17) with the ECD distribution given by (27) and boundary condition $m_0 = 0$. The solution (a) is the critical solution, while the solutions (b) and (c) are the two independent solutions obtained with $\eta = \frac{4}{5}\eta_c$ (see figure 1, and table 1 for numerical values). The ERN metric components $A^{-1} = B = (1 - m_\infty/r)^2$ are shown for corresponding m_∞ values (dotted lines).

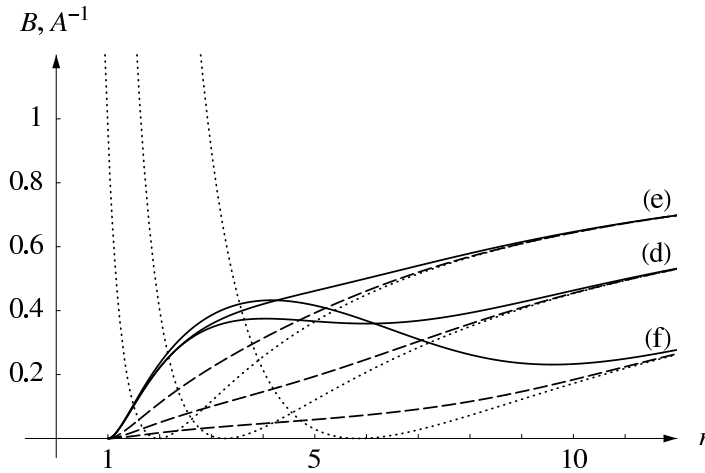


Figure 3. Regular spacetime metric components $g_{rr}^{-1} = A^{-1}(r)$ (thick lines) and $g_{tt} = B(r)$ (dashed lines) obtained by solving the field equation (17) with the ECD distribution given by (27) and boundary condition $m_0 = 1$. The solution (d) is the critical solution, while the solutions (e) and (f) are the two independent solutions are obtained for $\eta = \frac{4}{5}\eta_c$, (see figure 1, and table 1 for numerical values). The ERN profile functions $A^{-1} = B = (1 - m_\infty/r)^2$ are shown for corresponding m_∞ values (dotted lines).

The situation is substantially different for the solutions obtained with the boundary condition $m_0 > 0$. The metric components for the case $m_0 = 1$, labeled (d)–(f), in figure 1 and table 1, are shown in figure 3. At $r = m_0$, the metric component $A(r) = g_{rr}$ diverges ($1/A(r)$ reaches zero) which indicates an event horizon. When approached from $r > m_0$ the functions $1/A(r)$ and $B(r)$ appear to have a double zero at $r = 0$ and in this sense this spacetime singularity is equivalent to the ERN event horizon. Recall that at $r < m_0$ the spacetime metric is not specified by the solution to the field equation (17). This type of solutions we call singular.

For different choices of ECD distribution ρ , as for instance $\rho(R) \propto R^2 \exp(-R^2)$, basically the same bifurcating behaviour of solutions occurs. This fact will be used to simplify the treatment of ρ 's in section 5.

4. The δ -shell ECD distribution

Here we will consider the case of ECD distributed on a spherical shell of radius R_0 . A situation similar to this one was considered in [16], while thick shells were considered in [11]. We set

$$\rho(R) = \eta \delta(R - R_0). \quad (28)$$

Both in the interior ($R < R_0$) and in the exterior ($R > R_0$) space the general solution to (17) is of the form (21). We set the exterior solution to be asymptotically flat and allow the interior solution to be singular at $R = 0$:

$$U(R) = \begin{cases} k + m_0/R \equiv U_I, & R < R_0, \\ 1 + m_\infty/R \equiv U_E, & R > R_0. \end{cases} \quad (29)$$

The requirement that $U_I = U_E$ at $R = R_0$ fixes the value of k :

$$k = 1 + (m_\infty - m_0)/R_0. \quad (30)$$

Integration of the differential equation (17) with the rhs involving the δ -shell source (28) yields

$$R^2 U'|_{R-\epsilon}^{R+\epsilon} = -4\pi R_0^2 \eta U(R_0)^3. \quad (31)$$

When the solution (29) is substituted into the above relation the source strength η , m_0 , and the position of the δ -shell source, are interrelated:

$$\eta = \frac{m_\infty - m_0}{4\pi R_0^2} \left(1 + \frac{m_\infty}{R_0}\right)^{-3}. \quad (32)$$

This relation leads to bifurcating solutions similar to those discussed in section 3.

We now restrict the discussion to the regular solutions, i.e., we set $m_0 = 0$ and proceed with only one mass parameter $m = m_\rho = m_\infty$ given by equation (24). The source strength (32) is

$$\eta = \frac{1}{4\pi R_0} \frac{\xi}{(1 + \xi)^3}, \quad (33)$$

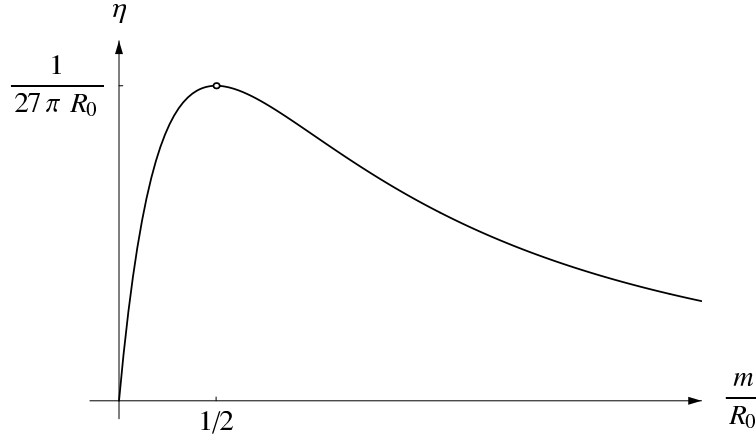


Figure 4. The source strength η vs. $\xi = m/R_0$ in regular solutions to the field equation (17) with δ -shell source (28).

where $\xi = m/R_0$ and it follows that at $\xi_c = 1/2$ there is a maximum $\eta_c = (27\pi R_0)^{-1}$ as shown in figure 4. For the regular solution the R -coordinate metric component $U(R)$ is

$$U(R) = \begin{cases} 1 + m/R_0, & R \leq R_0, \\ 1 + m/R, & R \geq R_0. \end{cases} \quad (34)$$

According to (18), the position of the δ -shell in the r -space is $r_0 = m + R_0$. In the interior of the δ -shell the r -space metric components are constants

$$A_I^{-1}(r) = 1 \quad \text{and} \quad B_I(r) = \left(1 - \frac{m}{r_0}\right)^2, \quad (35)$$

while in the exterior the metric follows the ERN metric given by (22). The metric components of only the critical regular solution involving the δ -shell ECD distribution are shown in figure 5.

5. Bifurcating behaviour and unified treatment of ECD distributions

Solutions for different ECD distributions $\rho(R)$ found in sections 3 and 4 exhibit bifurcating behaviour with respect to the source strength parameter η . When $\eta < \eta_c$, one is able to find two independent/different solutions to the same (nonlinear) differential equation with the same boundary conditions. As η approaches the critical value η_c the two solutions become identical. While the asymptotic flatness of the two independent solutions is fixed by the boundary conditions, their ADM mass (24) is different.

If one takes any m_∞ versus η curve in figure 1 (and corresponding spacetime metric component solutions), it is not possible to distinguish the upper branch from the lower branch solutions apart from m_∞ calculated from (24). Only a sequence of solutions provides a means to determine the branch along which solutions propagate.

One can expect that metric component configurations leading to smaller ADM mass when a mass source strength η is decreased are physically more acceptable than

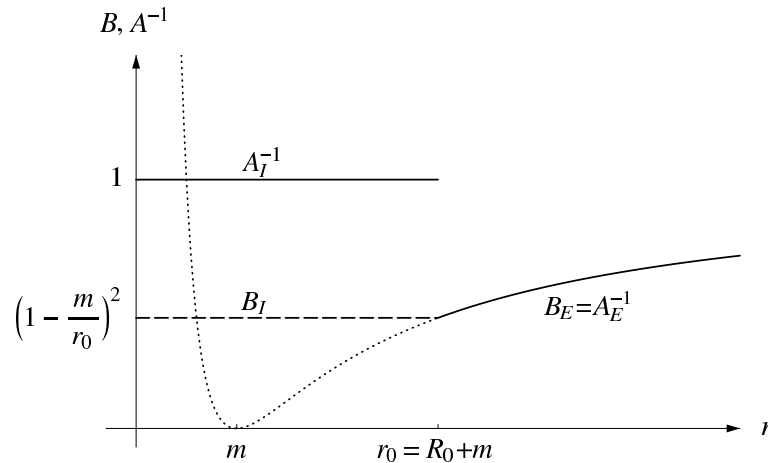


Figure 5. The metric components $g_{rr}^{-1} = A^{-1}(r)$ (thick line) and $g_{tt} = B(r)$ (dashed line) for the regular critical solution of the field equation (17) with δ -shell source (28). In the exterior of the shell located at $r_0 = m + R_0$, the metric is equivalent to the ERN (22) for the mass m (extended by dotted line into the interior space).

their counterparts which produce larger and larger mass $m_\infty = m_{\text{ADM}}$. Indeed, when the source strength is decreased from its critical value the low-mass bifurcation branch leads to classical (Newtonian gravity) configurations of ECD. One may say that the upper branch solutions (points (c), (f), (h) in figure 1) may tend to infinite mass which renders them to be (physically) unacceptable. Further investigation of stability properties of these solutions [17] might give some definite answer to the above assertions. On the other hand, the spacetimes corresponding to high-mass configurations have the interesting and important property of being quasi-singular which we discuss further in section 6.

Based on the bifurcation properties of the solutions to the field equation (17), we are going to introduce a normalization of the ECD distributions appropriate for the Majumdar–Papapetrou (MP) formalism. This will allow us to treat the diverse ECD distributions on equal footing and more easily explore their properties. We will focus only on the regular solutions, so only one mass parameter $m = m_\rho = m_\infty$ will be used. The ECD distributions considered in section 3 will be used to generate spacetimes that come arbitrarily close to having extremal horizons.

We first consider a general distribution $\rho(R) = \eta \rho_0(R)$ where η is the source strength factor and ρ_0 is normalized so that

$$4\pi \int_0^\infty R^2 \rho_0(R) dR = 1. \quad (36)$$

In the linear theory, the contribution of $\rho = \eta \rho_0$ to the total mass and charge of the configuration would be $m = q = \eta$, and there would be no upper bound imposed onto the source strength η (see figure 6, dotted line). In our case where the field equation (17) is non-linear, solutions exist only for values of η less or equal to a critical value η_c . For $\eta = \eta_c$ the solution is unique, we call it the critical solution, and we label

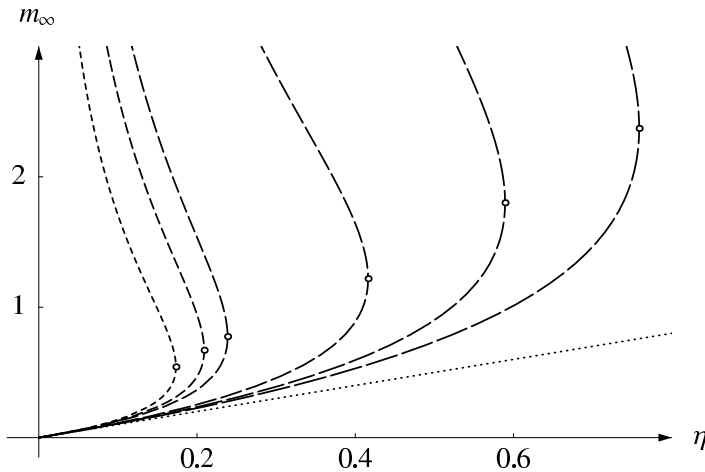


Figure 6. Dependence of mass m on the source strength η for the regular solutions to the field equation (17) with ECD distribution given by (37). Going from left to right, the tracks are ordered as in the table 2, critical solutions are indicated by circles. Dotted line indicates the expected behaviour in the linear theory.

the corresponding mass with the symbol m_c . For $\eta < \eta_c$ there are two independent, bifurcating solutions, leading to masses that we label m^\pm where it holds $m_- < m_c < m_+$.

As examples of ECD distributions normalized according to (36), we considered

$$\rho_0(R) = n(a, b) (R/\tilde{R})^a \exp(-(R/\tilde{R})^b), \quad (37)$$

where as before $\tilde{R} = 1$ (i.e. a unit mass), $a, b > 0$ are parameters and $n(a, b) = b/(4\pi\Gamma[(3+a)/b])$. The dependence of m on η for the parameter values $a = 0, 1, 2$ and $b = 1, 2$ is shown in figure 6. The numerical values for η_c and m_c are given in table 2. As can be seen, only the m^- -branch, and only at the low source strength limit, behaves as it would in the linear theory.

In the context of the field equation (17), we can formulate a more natural approach to normalization of the sources for the Majumdar–Papapetrou spacetimes that we will call MP-normalisation. For the MP-normalized ECD distribution $\hat{\rho}(R)$, we require that the critical source strength factor and corresponding mass are both equal to unity, i.e. $\eta_c = m_c = 1$. To obtain a MP-normalized ECD distribution starting from an arbitrarily normalized ECD distribution $\rho_0(R)$, we first solve (17) to obtain the values η_c and m_c . The MP-normalized source $\hat{\rho}$ is then constructed by rescaling the density ρ_0 according to (25) and (26) with the scaling parameter $\alpha = m_c$. The MP-normalized source $\hat{\rho}$ corresponding to ρ_0 becomes

$$\hat{\rho}(R) = m_c^2 \eta_c \rho_0(m_c R). \quad (38)$$

As an example we can take the δ -shell ECD distribution (28) discussed in section 4 for which we obtained $\eta_c = (27\pi R_0)^{-1}$ and $m_c = R_0/2$ (see figure 4). The MP-normalized δ -shell density follows as $\hat{\rho}(R) = (1/54\pi) \delta(R-2)$. In the case of the ECD distributions (37), the MP-normalized version reads

$$\hat{\rho}(R) = m_c^{a+2} \eta_c n(a, b) R^a \exp(-(m_c R)^b), \quad (39)$$

Table 2. The critical points in the regular solutions to (17) obtained with the with the ECD distribution (37).

a	b	$1/n(a,b)$	η_c	m_c
0	2	$\pi^{3/2}$	0.173 340	0.542 345
1	2	2π	0.209 013	0.670 181
2	2	$\frac{3}{2}\pi^{3/2}$	0.238 647	0.774 735
0	1	8π	0.416 177	1.218 82
1	1	24π	0.589 272	1.801 05
2	1	96π	0.758 753	2.371 19

where η_c and m_c obtained numerically are given in table 2.

The bifurcating solutions found in sections 3 and 4 have similar properties to the solutions found long time ago in another nonlinear field theory, i.e. in Yang–Mills gauge theory with external sources [18]. Stability of solutions has been investigated and different stability properties with respect to radial oscillations has been found [19, 20]. In the context of Einstein–Yang–Mills theory some of solutions have been found in the gravitating $SU(2)$ monopole context [21, 22, 23, 24] and an $SU(3)$ extension of this model [25], which could be characterized as bifurcating. Similar behaviour has recently been discussed in an extension of the Standard Model [26]. In some of the above papers the term bifurcation has been used rather loosely because some solutions found there do not follow the requirements from literature [15, 14]. Although an explanation of such behaviour is missing in all those works, a careful numerical analysis done in [21] as well as [27] offers an opportunity to compare solutions discussed before and bifurcating behaviour of our solutions.

We end this section by giving some technical details related to the numerical procedure we used to generate the bifurcating solutions: assume a sequence of solutions $f_i(x; \eta_i)$, $i = 1, 2, \dots$ to a nonlinear differential equation obtained with a sequence of source strength factors η_i . In order to find an expected upper or lower branch solution, when a solution is already found, one can replace the parameter η by a function $\eta(x)$ described by differential equation $d\eta(x)/dx = 0$. Since the system is now enlarged by one first order differential equation, one additional boundary condition has to be supplied. This boundary condition can be constructed from the functional value $f_k(x_s, \eta_k)$, by requiring that $\tilde{f}(x_s, \eta(x_s)) = f_k(x_s, \eta_k) \pm \delta f$, where $\tilde{f}(x, \eta(x))$ is a part of the enlarged system, and δf (being a small quantity) produces upper (+) or lower (−) functional value, giving an upper or lower branch solution. It is reasonable to choose $f_k(x_s, \eta_k)$ close to the critical value η_c . Once a solution is found the simple continuation used in the numerical code [13] could produce a corresponding sequence of solutions. Relative tolerances could be chosen to be very stringent (typical order is 10^{-6} to 10^{-8}) which assures that bifurcation is not produced by loose numerical boundaries and justifies the six significant digits given in table 2.

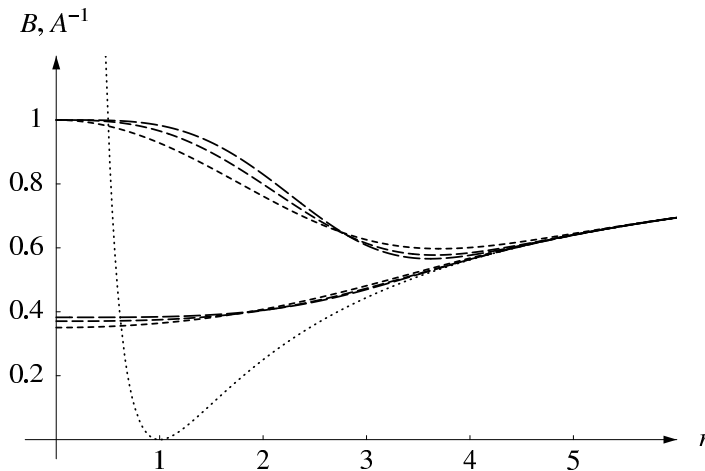


Figure 7. The r -space metric components $1/A$ and B (dashed lines) for the critical regular solutions obtained with the first three MP-normalized sources of figure 6 and table 2 (dashed lines), and for $m = 1$ ERN metric components (dotted line). (Also to be compared with metric components in figure 5.)

6. ECD distributions and quasi black holes

Using a MP-normalized ECD distribution $\hat{\rho}$, the critical regular solution to the field equation (17) is obtained with the source strength $\eta = \eta_c = 1$. The r -coordinate metric components of the critical regular solutions to (17) and the ECD distribution (39) with parameters $a = 2$ and $b = 0, 1, 2$ are shown in figure 7. At large r , metric components A and B coalesce into the $m = 1$ ERN metric, while at the intermediate values where major part of the ECD is distributed, they are manifestly regular and do not show significant dependence on the choice of the shape of the ECD distribution. By using $\eta < 1$, these solutions can, due to the bifurcating behaviour, either evolve toward flat space along m^- branch, or toward higher mass configurations along the m^+ branch. Any of these solutions can be rescaled to describe a unit mass configuration if the rescaling according to (25) and (26) is carried out with the scaling parameter $\alpha = m$. Starting from the critical solutions shown in figure 7 we followed the m^+ -branch to obtain the field configurations corresponding to $m^+ = 10$ and $m^+ = 100$ which we then rescaled to restore the unit mass configurations. The metric components of these solutions are shown in figure 8.

It is plausible that, by following the m^+ -branch toward higher masses and then rescaling the solutions to describe the $m = 1$ configurations, the minimum of the function $1/A(r)$ is deeper and closer to $r = 1$. Asymptotically, in the region $r > 1$ the metric components $A(r)$ and $B(r)$ follow the ERN metric and as the point $r = 1$ is approached from $r > 1$ there appears to be a double zero both in $1/A(r)$ and $B(r)$. In the $r < 1$ region we would asymptotically have $B = 0$ which would not allow for timelike intervals. However, since our spacetimes are regular everywhere and such a situation is realized only asymptotically, we can consider a radially moving photon for which $ds^2 = 0$ and

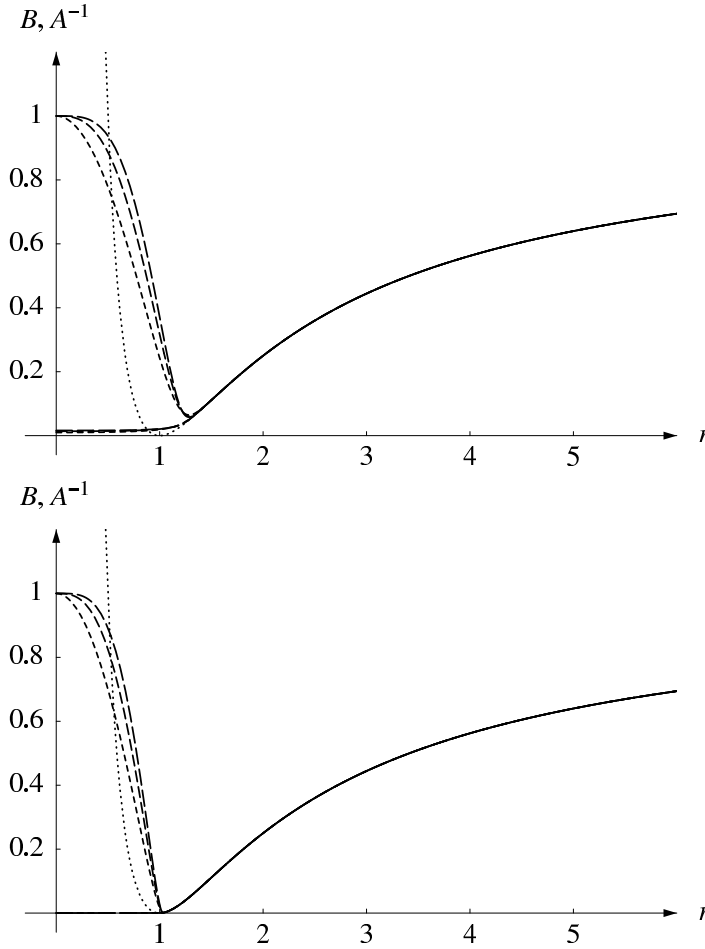


Figure 8. The r -space metric components obtained by using the MP-normalized sources as in figure 7 to generate $m^+ = 10$ (upper panel) and $m^+ = 100$ (lower panel) regular solutions which were then rescaled to describe unit mass objects. $m = 1$ ERN metric (dotted line).

$d\omega^2 = 0$, so $dt/dr = \pm\sqrt{A/B}$. The ratio of the metric components $\sqrt{A/B}$ for the $m^+ = 10$ /rescaled solutions, related to the time required for the photon to transverse a unit distance in the r -coordinate, is shown in figure 9.

The distributions of the ECD for the solutions of figure 8 are shown in figure 10. Asymptotically, as we would go higher on the m^+ -branch and rescale to restore unit mass configurations, the density would be completely pulled within the $r = 1$ region. The same was obtained by [10].

7. Conclusions

The Majumdar–Papapetrou formalism provides a good environment to study solutions to Einstein–Maxwell equations where matter is assumed to be described by electrically counterpoised dust (ECD). In this paper, we have obtained and analyzed regular and quasi black hole solutions stemming from the M–P formalism and obtained for diverse

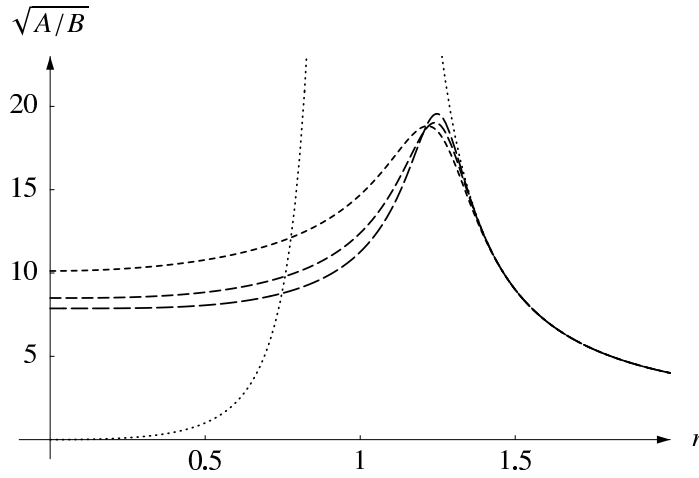


Figure 9. The ratio $\sqrt{g_{rr}/g_{tt}} = \sqrt{A(r)/B(r)}$ for the solutions shown in figure 8 (dashed lines) and for the ERN metric (dotted lines).

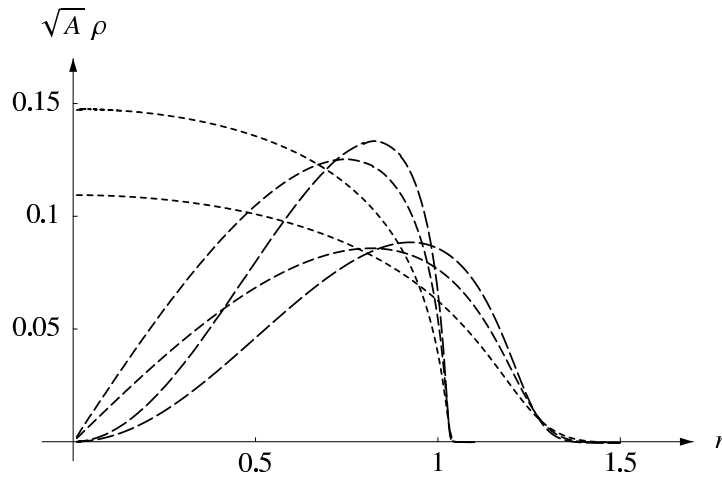


Figure 10. The density $\sqrt{A}\rho(r)$ for the solutions in figure 8. The densities that effectively vanish at $r \simeq 1.1$ correspond to $m^+ = 100/\text{rescaled}$ solutions, while those that effectively vanish at $r \simeq 1.5$ correspond to $m^+ = 10/\text{rescaled}$ solutions.

spherically symmetric ECD distributions by numerical integration of the nonlinear field equations. As an immediate consequence of nonlinearity, bifurcating solutions have been identified with respect to the amount of ADM mass allocated in the mass source term. Also an upper bound to the source strength has been found above which no solution exists. Although ECD distributions have assumed analytically different (spherically symmetric) forms, we have been able to reformulate the sources to treat them on equal footing. From this treatment we have been able to obtain regular solutions that come arbitrarily close to black hole solutions, the so called quasi black holes. Investigation of such bodies could be useful in investigations of interiors of black holes that still hide many unanswered questions. Bifurcation is not an unusual feature in gauge field theory [19] or in gravity [24, 23]. It is encouraging that here we are able to show

that the bifurcation described in this work is not an artifact of a particular choice of charge/matter/energy density. Stability and bifurcation are closely related problems, so investigation of the above solutions with regard to stability is a natural extension of this work, bearing in mind the citation from Ref. [15] ‘... stability analysis may be more expensive than the calculation of the solutions themselves.’

Acknowledgments

This work is supported by the Croatian Ministry of Science and Technology through the grant ZP 0036038. Authors would like to thank for hospitality the Abdus Salam International Centre for Theoretical Physics, Trieste, Italy, where part of this work was carried out.

References

- [1] Bonnor W B and Wickramasuriya S B P 1975 *Mon. Not. R. Astron. Soc.* **170** 643
- [2] Bonnor W B and Wickramasuriya S B P 1972 *Int. J. Theor. Phys.* **5** 371
- [3] Bonnor W B 1998 *Class. Quantum Grav.* **15** 351
- [4] Oppenheimer J R and Snyder H 1939 *Phys. Rev.* **56** 455
- [5] Majumdar S D 1947 *Phys. Rev.* **72** 390
- [6] Papapetrou A 1947 *Proc. R. Ir. Acad. Sect. A* **51** 191
- [7] Papapetrou A 1954 *Z. Phys.* **139** 518
- [8] Varela V 2003 *Gen. Rel. Grav.* **35** 1815
- [9] Bonnor W B 1999 *Class. Quantum Grav.* **16** 4125
- [10] Lemos J P S and Weinberg E J 2004 *Phys. Rev. D* **69**, 104004
- [11] Kleber A, Zanchin V T and Lemos J P S 2004 *Preprint* gr-qc/0406053
- [12] Bonnor W B 1960 *Z. Phys.* **160** 59
- [13] Asher U, Christiansen J and Russel R D 1981 *ACM Trans. Math. Softw.* **7** 209
- [14] Hagedorn P 1988 *Non-linear oscillations* 2nd. ed. (Oxford: Clarendon Press)
- [15] Seydel R 1988 *From Equilibrium to Chaos – Practical Bifurcation and Stability Analysis* (New York: Elsevier)
- [16] Gürses M 1998 *Current Topics in Mathematical Cosmology* (Singapore: World Scientific) p 425
- [17] Horvat D and Ilijić S submitted to *Fizika B (Zagreb)*
- [18] Jackiw R, Jacobs L and Rebbi C 1979 *Phys. Rev. D* **20** 474
- [19] Jackiw R and Rossi P 1980 *Phys. Rev. D* **21** 426
- [20] Horvat D 1986 *Phys. Rev. D* **34** 1197
- [21] Breitenlohner P, Forgács P and Maison D 1992 *Nucl. Phys. B* **383** 357
- [22] Brihaye Y, Hartmann B and Kunz J 2000 *Phys. Rev. D* **62** 044088
- [23] Lue A and Weinberg E J 1999 *Phys. Rev. D* **60**, 084025
- [24] Brihaye Y, Grard F, and Hoorelbeke S 2000 *Phys. Rev. D* **62** 044013
- [25] Brihaye Y and Piette B M A G 2001 *Phys. Rev. D* **64** 084010
- [26] Brihaye Y *Preprint* hep-th/0412276
- [27] Brihaye Y, Hartmann B and Kunz J 1998 *Phys. Lett. B.* **441** 77